

# Innovative Processing for Power Factor and Efficiency Improvement of LSPM Considering Inductance of Rotor Structure

S. Saha, S.I. Byun, Y.H. Cho

Department of Electrical Engineering, Dong-A University  
Busan, South Korea

**Abstract**--Recently Line Start Permanent Magnet Machine (LSPM) is a well-known motor due to its technical advantages in academic and industrial sector. The LSPM combines a permanent magnet rotor that allows higher motor efficiency during synchronous operation, and an induction motor squirrel cage rotor for starting the motor by connecting it directly to an A.C. Source. Such a construction generates important technical advantages like reduced manufacturing costs and better performances. In this paper, we will deal with the efficiency and Power factor improvement of a 3.4kW, 2-pole, three-phase LSPM using the difference in d-axis magnetic inductance ( $L_d$ ) and q-axis magnetic inductance ( $L_q$ ). d-axis and q-axis magnetic inductance are nonlinear problem which are varied with current level and current angle. Therefore, nonlinear finite element analysis is necessary to obtain the  $L_d$  and  $L_q$ . The efficiency improvement can be effectively achieved by designing optimization of the rotor structure using finite element method. The optimized slot shape of PM was selected for the prototype machine, which improves the efficiency and power factor of LSPM.

**Keywords**--LSPM; inductance; rotor structure; efficiency; power factor; FEA

## I. INTRODUCTION

Recently due to the demand of energy saving purpose, replacement of the line-operated induction motor (IM) by line start permanent magnet synchronous motor (LSPM) is of concern in both academy and industry. LSPM has a higher efficiency than (IM) and an advantage in constant speed operation regardless of the effect of load variation, presenting an interesting alternative for IMs in pumping systems. It has permanent magnets (PMs) buried below the squirrel cage in rotor, thus operates in steady state as conventional interior permanent magnet synchronous motor (PMSM); the squirrel cage is used for line starting on a conventional AC power source and damping of dynamic oscillations at fast load changes. Thus it combines the advantages of induction motor (robust construction and line-starting capability) and PMSM (high efficiency, power factor). The line start permanent magnet motor (LSPM) is noted as alternative routes comparing with the induction motor that it offers high efficiency and unity power factor. The LSPM motor has widely been used in household appliance such as the compressor of air-condition and refrigerator. LSPM shows operating characteristics that

have directly from the commercial electricity without additional power electronic switching devices. [1]- [2]

In this paper, we will deal with the efficiency and Power factor improvement of a 3.4kW, 2-pole, three-Phase line start permanent magnet synchronous motor (LSPM) using the difference in d-axis inductance ( $L_d$ ) and q-axis inductance ( $L_q$ )[4]. The efficiency improvement can be effectively achieved by designing optimization of the rotor structure using the response surface method and finite element method [3]. The optimized slot shape of PM was selected for the prototype machine shows in Fig. 1, which improves the efficiency and power factor of LSPM. Finally the performance characteristic of the designed model is compared with that of the initial model. A 3.4kW three phase LSPM motor was designed and optimized in this paper. Table 1 shows the design specification. It is a three-phase two pole machine; each pole has three pieces of PMs as shown in Fig.1. The cage on rotor is made by aluminium die-casting, and PMs are then inserted into groove of rotor core. Material of permanent magnet is Nd-Fe-B, and residual flux density and coercive force are  $=1.21\text{T}$  and  $=735\text{ kA/m}$ , respectively. Therefore the design variables are limited when selecting design variables.

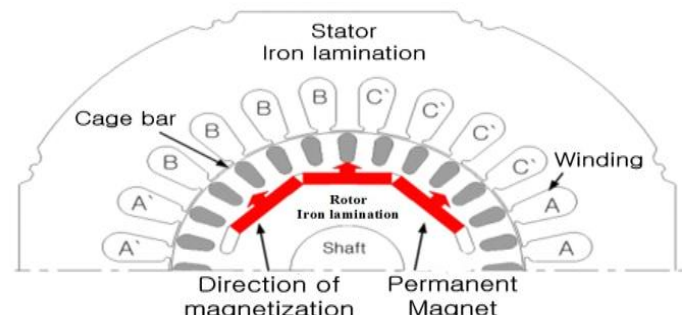


FIGURE 1. LSPM MODEL STRUCTURE.

TABLE I. DESIGN SPECIFICATION OF LSPM.

Item	Value	Item	Value
Phase	3	Rotor Outer Diameter [mm]	87.8
Pole Number	2	Rotor Inner Diameter [mm]	25.4
Rated Torque [Nm]	9.1	Rotor bar number	28
Rated Speed [rpm]	3600	Rotor bar material	Aluminum
Frequency [Hz]	60	Material of magnets	Nd-Fe-b
Stator Outer Diameter [mm]	159	Stack Length [mm]	90
Stator Inner Diameter [mm]	89	Br at 100°C [T]	1.21
Lamination [mm]	90	Hc at 100°C [KA/m]	7.35
Slots number	24	Thickness [mm]	3

## II. ANALYSIS OF STEADY STATE

The LSPM has superior torque characteristic since the PMs and conductor bars are buried in rotor core. Therefore, the LSPM has the beneficial attributes of both interior-PM (IPM) motor and induction motor [5], that it generates synchronous starting torque by means of an induction rotor cage, when running synchronously in steady state. Electromagnetic torque  $T_e$  of LSPM machine expressed as:

$$T_e = \frac{3}{2} \frac{P}{2} (\lambda_{pm} i_q - (\xi - 1) L_d i_d) i_q \quad (1)$$

Where,  $i_d$  and  $i_q$  are the components of armature current.  $L_d$  and  $L_q$  are the d-axis and q-axis inductances,  $\lambda_{pm}$  is the PM flux linkage and P is number of poles and  $\xi$  is saliency ratio.

$$L_q = \frac{\psi_0 \sin \alpha}{i_q} \quad (2)$$

$$L_d = \frac{\psi_0 \cos \alpha - \psi_a}{i_d} \quad (3)$$

$$\xi = \frac{L_q}{L_d}$$

Where,  $i_d = -I_a \sin \beta$  and  $i_q = I_a \cos \beta$ .

## III. OPTIMIZATION OF LSPM

The original model of this machine is shown in Fig.2, and the analysis and experimental results have been reported in [6]. The block PM used in the original model has a thickness of 3 mm and length of 28 mm. Statistical experimental methods such as design of experimental (DOE) and response surface methodology (RSM) have been applied to optimize media for industrial purposes. RSM is a collection of statistical techniques for designing experiments, building models, evaluating the effects of various factors and searching for the optimum conditions. It is applied to determine an optimization structure of permanent magnet slot in LSPM rotor.

Three design variables in this optimization process are chosen as illustrated in Fig. 3: the length from PM slot to shaft L, air duct gap Rib and slop angle of side PM  $\theta$ . Thickness of PM is fixed at 3 mm due to de-magnetization weakness during synchronization. The length from PM slot to shaft is chosen from 8.80 mm to 16.72 mm, air duct gap is constrained to 2 to 2.40 mm, and slip angle of side PM is 135 to 147 degree. Ranges of them are listed in Table II. Therefore, when the angle increases, the inverse relationship L, and Rib are reduced. In addition, Fig.9 shows power factor according to  $\theta$  angle. The  $\theta$  angle increases when the magnet and the value of L are reduced. Therefore power factor is getting higher as well as efficiency. The power factor and efficiency equations are given below.

$$PF = \cos(\varphi) = \cos \left( \tan^{-1} \left( \frac{\frac{L_d i_d + i_q}{L_q i_q + i_d}}{\frac{L_d - 1}{L_q}} \right) \right) = (\xi - 1) \sqrt{\frac{\sin(2\alpha)}{2(\tan \theta + \xi^2 \cot \alpha)}} \quad (4)$$

$$\eta = \frac{P_{Out}}{P_{Out} + P_{Loss}} = \left( 1 + \frac{1}{\frac{\omega_r}{3R_{th}} \left( \frac{T}{I^2} \right)} \right)^{-1} \quad (5)$$

Here,  $P_{Loss} = 3R_{th} I^2$ ,  $\xi$  is the machine saliency ratio,  $\alpha$  is the current angle,  $I$  is the line current,  $T$  is the electromagnetic torque,  $R_{th}$  is total resistance,  $\omega_r$  is the mechanical angular velocity,  $\eta$  is the efficiency of LSPM.

TABLE II. DESIGN VARIABLES AND EXPERIMENT RANGE FOR RSM.

Design variable	Item of design variable	Experiment range	Unit
$L$	Length from PM slot to shaft	[8.80~16.72]	[mm]
$\theta$	Slot angle of side PM segment	[135°~147°]	[deg]
$Rib$	Air duct gap	[2~2.40]	[mm]

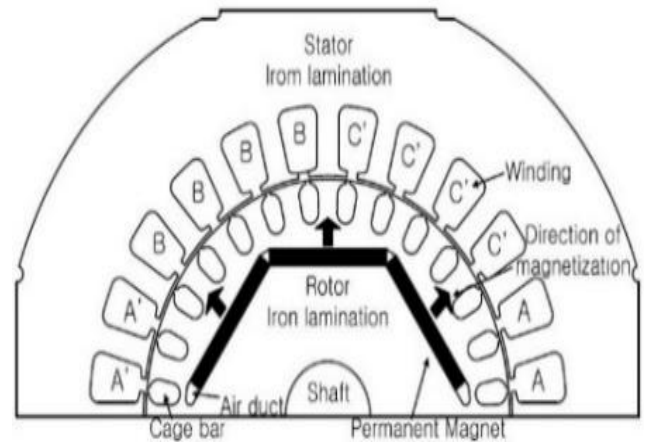


FIGURE II. ORIGINAL MODEL OF LSPM.

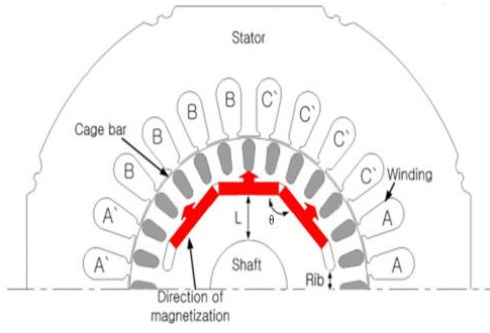


FIGURE III. OPTIMAL STRUCTURE OF MODIFIED LSPM MODEL.

First, design candidates with  $L$  (8.80~16.72 mm),  $\theta$  ( $135^\circ$ ~ $147^\circ$ ) and Rib (2~2.40 mm) were studied by transient finite element analysis. The response surface of efficiency of minimum current is given in Fig.4. Optimum candidate  $L=8.80$  mm,  $\theta=147^\circ$ , Rib=2.37 are satisfied with the efficiency and power factor. With 85% amount of PM material and same aluminum material used in the original model, the final model of LSPM is analyzed and manufactured according to the optimal PM groove design.

#### IV. VERIFICATION AND EXPERIMENTAL TEST

In this paper, finite element analysis of a LSPM was carried out using the commercial software Maxwell. The original model and optimized mode were analyzed in order to verify the optimization and further study the performances. The optimized model was designed with same stator core and winding. Performance such as torque ripple, power factor and efficiency are studied first. It could be found that torque ripple for optimized model is about 40% smaller than the original model. A reduction of 40% in torque ripple means more smooth torque as well better performance of the motor.

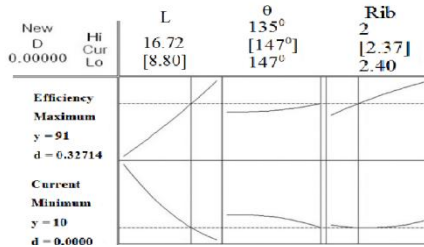


FIGURE IV. OPTIMIZATION ANALYSIS WITH RSM.

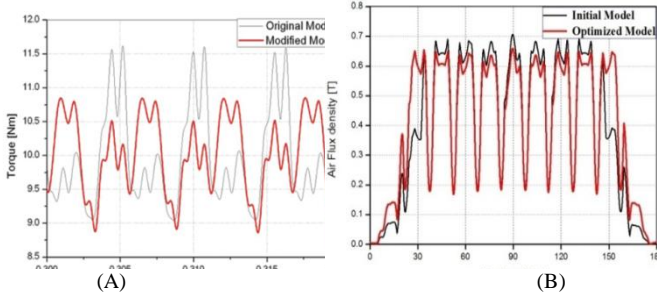


FIGURE V. (A) TORQUE RIPPLE AT FULL LOAD OPERATION (B) COMPARISON OF AIR-GAP FLUX DENSITIES.

Adjust of Slot angle of side PM segment ( $\theta$ ) and length of  $L$  would obtain a more sinusoidal air gap flux density waveform. Comparison of the air-gap flux density waveforms for the motor at no load condition are given in Fig. 5 (b). It is obvious that the optimized model is able to offer a large peak air-gap flux density than the original motor and the shape of the curve is more like an ideal sinusoidal curve. The  $\theta$  angle increases when the magnet and the value of  $L$  are reduced. Consequently  $q$ -axis reluctance tend to be smaller, when  $L_q$  is getting increased by securing area between the magnet slots and the conductor bar. In addition, Fig.6 and Fig. 7 shows  $q$ -axis and  $d$ -axis inductance according to  $\theta$  angle respectively. In this paper, size and trends have changed significantly depending on design variable. Rib is an important variable to improve performance of LSPM. Whether Rib size is smaller, the magnetic torque is greater causing leakage of magnetic flux decreases. Due to the  $q$ -axis flux flow reluctance torque and  $q$ -axis inductance are decreases respectively. On the other hand, with large rib size, magnetic torque is reduced and leakage of magnetic flux is increases. In case of  $L$ , permanent magnet moves closer to the shaft, it confirmed that the  $q$ -axis inductance was increased.

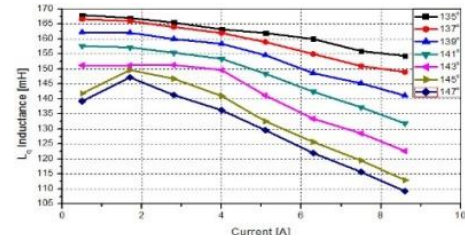


FIGURE VI. Q-AXIS INDUCTANCES ACCORDING TO THE  $\theta$  ANGLE.

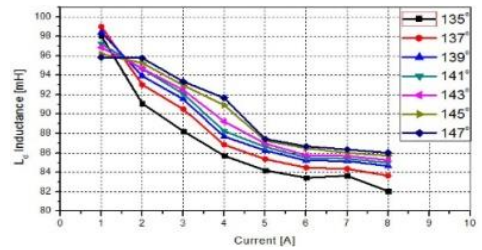


FIGURE VII. D-AXIS INDUCTANCES ACCORDING TO THE  $\theta$  ANGLE.

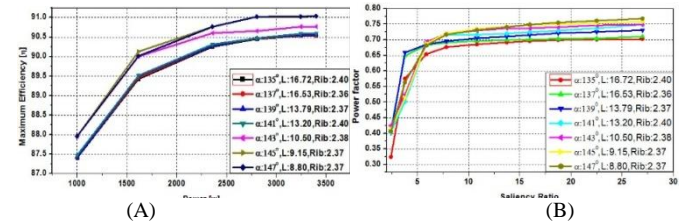


FIGURE VIII. (A) EFFICIENCY CURVE AT RATED POWER (B) POWER FACTOR AND SALIENCY RATIO CURVES ACCORDING TO  $\theta$  ANGLE.

The efficiency and power factor waveform influences the performance of motor seriously. The efficiency and power factor waveform of the proposed model are calculated for different variables. The waveform are shown in Fig. 8 (a), (b) which represents when the angle increases, the inverse relationship L, and Rib are reduced and efficiency and power factor also increases respectively. Comparison results depicted in Table. III. From the comparison results it can be decided that the value of  $\theta$  angle increases when the magnet and the value of L are reduced. Thereby power factor and efficiency are increasing. Efficiency appear to be same for  $\theta = 145^\circ \sim 147^\circ$  although power factor little bit increase for  $\theta = 147^\circ$ . Therefore,  $\theta = 147^\circ$ ,  $L=8.80$ ,  $Rib=2.37$  are predict as an optimal value which is fully satisfied with RSM prediction.

TABLE III. DESIGN VARIABLE OF MAGNET POLE SHAPE.

$\theta$ [deg.]	L [mm]	Rib [mm]	Power factor	$\eta$ [%]
$135^\circ$	16.72	2.3880	0.7025	90.54
$137^\circ$	16.53	2.3679	0.71	90.55
$139^\circ$	13.79	2.3696	0.7305	90.56
$141^\circ$	13.20	2.3960	0.7484	90.59
$143^\circ$	10.50	2.3794	0.7485	90.77
$145^\circ$	9.15	2.3697	0.7575	91.0321
$147^\circ$	8.80	2.3703	0.76785	91.0441

## V. EXPERIMENTAL RESULTS

LSPM with optimized rotor has been prototyped for the experimental validation of the FEA results and the verification of the rotor optimization techniques. Experiment was set up to test the prototype motors using dynamo test bed as shown in Fig.10. Fig. 9 shows the photo of optimized rotor. Load test at rated speed (3600 rpm) are carried out by varying load factor from 0 to 120 [%]. Power, phase current, efficiency and power factor according to different load were recorded and summarized in Fig. 11. The performance curves according to different load torque at rated speed, 3600 rpm was summarized in Fig.11 confirmed that FEM analysis and experimental data are almost identical as shown in Table IV. The simulation and experimental results are compared according to rated voltage, rated current, rated speed, rated torque, efficiency, which represents the accuracy and the results obtained shows very good agreement.

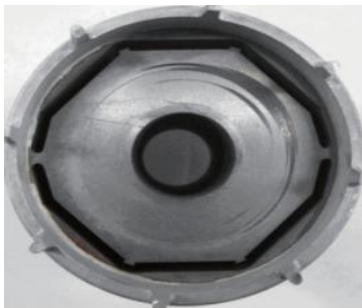


FIGURE IX. OPTIMIZED ROTOR.

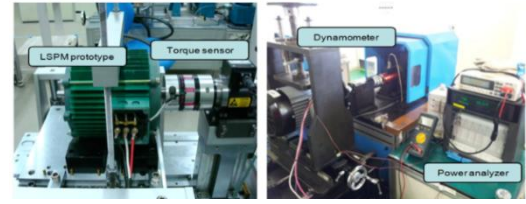


FIGURE X. DYNAMO SETUP TO TEST OF LSPM.

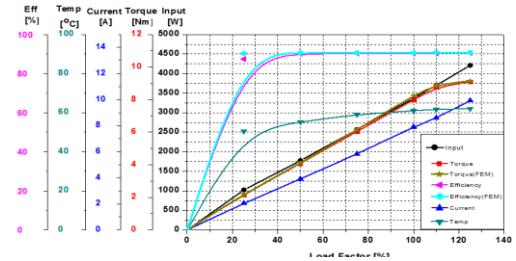


FIGURE XI. PERFORMANCE CURVES AT RATED SPEED.

TABLE IV. COMPARISON BETWEEN EXPERIMENT AND FEM RESULT.

Items	Unit	FEM	Experiment
Rated Voltage	[V]	380	380
Rated Current	[A]	10	10
Rated Speed	[rpm]	3600	3600
Rated Torque	[Nm]	9.177	9.17
Efficiency	[%]	91.044	91
Output	[W]	3400	3400

## VI. CONCLUSION

This paper describes the development process of a 3-Phase 3.4kW 2-Pole LSPM by optimizing the rotor structure using response surface method. Two-dimensional transient finite element analysis was utilized for accurate calculation of efficiency, current, speed curve etc. The experimental results obtained from the prototype demonstrate satisfactory agreement with the estimated by FEA approaches, and underpin the findings of the study. And optimum design for the rotor is satisfied with the required motor specification. Therefore through the inductance, motor about power factor and efficiency could be seen improvement.

## ACKNOWLEDGMENT

This research was supported by the National Research Foundation of Korea (NRF) grant funded by the Korea Government (MSIP) No: NRF- 2014R1A2A2A01003368 and by the Human Resources Development of the Korea Institute of Energy Technology Evaluation and Planning (KETEP) grant funded by the Ministry of Knowledge Economy, Republic of Korea under Grant 20134030200320.

## REFERENCES

- [1] M.A Rahman and T.M. Osheiba, "Performance of a large line start permanent magnet synchronous motor", *IEEE Trans. Energy Conversion*, vol. 5, pp.211-217, mar. 1990
- [2] T.J.E. Miller, "Synchronization of line-start permanent magnet AC motor," *IEEE Trans. Industry application*, vol. PAS-103, 1984, pp.1822-1828

- [3] F.J.H.Kalluf, C.Pompermaier, M.V.F da Luz and N.Sadowski, Magnet flux optimization method for line start permanent magnet motors, IEEE International Electric Machines and Drives, May 2009, 953-957.
- [4] T.J.E. Miller, "Single phase permanent magnet motor analysis," IEEE Trans. Industry application, IA-21 (4) (1985), 651-658.
- [5] C.A.da Silva, J.R. Cardoso and R. Carlson, "Analysis of a three-phase LSPMM by numerical method," IEEE Trans. On Magn., vol.45, (March 2009), 1792-1795
- [6] J. Li and Y.H. Cho, "Design of high performance line start permanent magnet synchronous motor with high inertia load," International Journal of Applied Electromagnetics and Mechanics 33 (1, 2) (2010), 621-628.